NASA CR-54121

THE THERMAL ANALYSIS OF ANODE AND CATHODE REGIMES IN AN ELECTRIC ARC COLUMN

by

E. Pfender, S. Wutzke, G. Gruber, and E.R.G. Eckert

prepared for

NATIONAL AERONAUTICS AND SPACE ADMINISTRATION

HEAT TRANSFER LABORATORY

MECHANICAL ENGINEERING DEPARTMENT

UNIVERSITY OF MINNESOTA

Requests for copies of this report should be referred to:

National Aeronautics and Space Administration
Office of Scientific and Technical Information
Washington 25, D.C.
Attention: AFSS-A

NASA CR-54121

QUARTERLY PROGRESS REPORT No. 7

(January 1, 1965 to March 31, 1965)

THERMAL ANALYSIS OF ANODE AND CATHODE REGIMES IN AN ELECTRIC ARC COLUMN

by

E. Pfender, S. Wutzke, G. Gruber, and E.R.G. Eckert

Prepared for

NATIONAL AERONAUTICS AND SPACE ADMINISTRATION

April 15, 1965

CONTRACT NAS 3-2595

Project Manager
NASA - Lewis Research Center
Cleveland, Ohio
Spacecraft Technology Division
James Sovey

HEAT TRANSFER LABORATORY
DEPARTMENT OF MECHANICAL ENGINEERING
UNIVERSITY OF MINNESOTA
MINNEAPOLIS, MINNESOTA

INTRODUCTION

The Heat Transfer Laboratory at the University of Minnesota is engaged in a program of theoretical and experimental investigation of heat transfer phenomena occurring in electric arcs under NASA Contract No. NAS 3-2595. The project manager for this contract is Mr. J. Sovey of the Electrothermal Technology Section, Lewis Research Center.

This report covers work performed during the period from January 1, 1965 to March 31, 1965. This seventh reporting period was primarily devoted to performing experiments with the segmented anode covering electrical as well as thermal measurements. In addition, both a double anode and a cylindrical anode were designed and constructed. The construction of the plasmascope was also completed and some preliminary tests in a hydrogen atmosphere were performed.

Experiments with Segmented Anode

During this period the technique applied for electrical measurements with the segmented anode was improved. Thus, it was possible to study the behavior of the arc over a wide range of parameter settings. The knowledge of the current distribution is important for the heat transfer to the anode because it is suspected that the current causes the main contribution to the anode heat flux. These current measurements will permit us to determine separately the amount of heat transferred to a particular segment due to the current flux. Results of such measurements are shown in Figs. 3-6. For a wide electrode gap, atmospheric pressure, and a high blowing rate, the arc will be extinguished (Fig. 5) because of the limited open-circuit voltage. In the other extreme, for a small gap, low pressure, and low blowing rates, the arc operates only in the steady mode. The corresponding oscillogram does not show anything but straight lines and therefore no pictures were included.

The 6 traces on the oscillograms, starting at the top, show the individual currents through 4 consecutive segments and the total current as DC signals, and the overall voltage as an AC signal. The 4 consecutive current carrying segments were in all cases the first through fourth segment downstream from the cathode tip except for the following settings where the second through fifth segments were involved: S = 9 mm, I = 100 Amps for both, P = 760 torr, V = 30 and 60 m/sec, and P = 380 torr, V = 60 and 100 m/s.

The oscillograms show that the total current remains constant in spite of the arc fluctuations. This feature seems to a large extent to be due to the characteristic of the power supply which exhibits a high inductive impedance. Therefore, no sudden current change is possible, and the restriking of the arc shows up only as a sudden voltage drop. In some oscillograms, however, the current traces show a small fluctuation in the signal when restriking occurs. This was due to a capacitance which was later found in the arc starting circuitry. Since it was removed this effect did not appear any more in recent measurements.

The traces of the individual segment currents, using the grid lines of the oscilloscope screen as zero reference, show two significantly different shapes of the increasing current. A nearly exponential increase indicates restriking at that particular segment, while a linear increase appears with a transition of the arc attachment point from an adjacent segment upstream. The current decrease is shaped complementarily since the total current cannot change. A linear decrease indicates the current transition to an adjacent segment downstream; an exponential decrease is caused by a decaying plasma column far downstream. Restriking did not always occur at the first segment, and the current distribution was also in most cases more irregular. The oscillogram for P = 760 torr and V = 30 m/s in Figure 3 is an example for both situations. The first cycle shows restriking of the arc at the first segment, regular transition to segments two, three, and four, and arc decay in segment four. In the following cycle the arc restruck at the second segment with a regular transition to the third segment, decayed partially at this segment already while again restriking at the second segment occurred. However, before the current reached the maximum value, the arc restruck at the first segment and before being fully developed, passed over to the second segment again, which finally drew the total current. All instantaneous individual segment currents, however, add up to a constant total current.

Considering the restrike process, one can divide the exponential current increase into a steep breakdown part and a remaining "channel development" part, indicated by a gradual current increase. The time required for breakdown was in all cases $80 \pm 40\ \mu s$. It is assumed that the voltage between the plasma column and an anode segment leads to the development of electron avalanches which finally cause the breakdown.

The traces of the individual segment currents show that the time interval required for the anode arc terminus to travel across the 0.010 inch layer of mica separating each segment is somewhat longer than one would expect from the average speed across the 1/2 inch segment. This indicates that the edges of the segments are preferred attachment points.

The mean velocity determined from these electrical measurements is in agreement with those obtained from the evaluation of the high speed movies. This mean velocity was always found to be smaller than the blowing velocity. The difference between these two velocities increases with decreasing current, increasing blowing velocity, increasing gap width, and decreasing pressure.

A further attempt has been made during this reporting period to measure the voltage required for restriking the arc. The current leads for all but one of the segments were disconnected to keep the anode arc attachment point fixed to one particular segment. The dynamic measurement of a restriking arc characteristic was found possible by using an oscilloscope. However, the data, especially the breakdown potential itself, were not reproducible enough. The reason for this is apparently the continuous deposition of contaminations on the anode surface. An attempt was made to establish at least equal initial conditions for these experiments.

Symmetrical Double Anode

During this reporting period a new double anode assembly, which is symmetrical at the inlet, was designed and constructed. This anode configuration consists of two plane anodes which are situated opposite each other in the top and bottom of the test section, respectively. The new design which is shown in Figure 1 permits one to vary the amount of separation between the two anodes by putting in various shim thicknesses.

The two anodes are electrically insulated from the test section so that the current through each anode can be measured independently. A separate current shunt is attached at one end to each anode and at the other end to a common lead from the positive terminal of the power supply which is grounded. Thus, the two anodes are kept at the same potential. The two anodes also have their own water circuits which permit a separate measurement of the total energy flux to each anode calorimetrically. The distance between the two anodes can presently be set at either 5, 10, or 15 mm.

The new design should eliminate the problem of unsymmetrical flow mentioned in the last quarterly report.

Cylindrical Anode

A cylindrical anode assembly was also designed and constructed during this reporting period. As shown in Figure 2, this anode is inserted into the existing test section from the top by means of a special brass holder. The holder has a smooth entrance region machined into it. The anode proper consists of a copper insert. The inside diameter of the anode can be readily changed by installing different size inserts. Presently, 1/8, 3/16, and 1/4 inch ID inserts are available.

The cylindrical anode will be used for comparison purposes to check the equivalency of the data from the plane anode to that obtainable from cylindrical geometries. In addition, it will provide design information for the segmented, cylindrical anode which is planned for the future.

Plasmascope

The construction of the optical system for spectrographic measurements (plasmascope) proceeded as planned. The optical components ordered, have arrived and have been attached to the supporting members made in our shop. The one exception is the 1/4 wavelength, coated calibration arc mirror which should arrive shortly. Assembly of the plasmascope was completed using a calibration mirror of lesser quality.

The plasmascope was aligned using the usual point light source and also a laser. The laser greatly facilitated the location of the optical benches.

While checking the optical system for distortion, we found that some of the front surface aluminum mirrors were not flat enough for a clear picture of the object. Rearranging and substituting some spare flatter mirrors minimized the effect to an acceptable level for now. In the future we will get mirrors flat to at least 1/2 wavelength.

As the distortion was reduced, we become aware of small vibrations in the system. The arc cathode and the optical pick-up system vibrate slightly. The arc tunnel blower and the vacuum pump are the main cause of vibration, although other motors contribute too. The largest vibration is in the cathode which has a cantilever type suspension. Though the vibrations are small, we hope to reduce them further.

The optical system has been checked for uniformity of intensity across the slit when a uniform light source is viewed. The intensity varied only ± 2% over the slit height of 1.9 cm, neglecting amplifier delay time. The source was a white screen illuminated by a projector such that only the diffuse light was gathered by the plasmascope.

The useful wavelength range of the optical system was measured with both a blue and red sensitive photomultiplier tube. The anode of a carbon arc was used as the source. The ratio of the intensity measured to the calculated intensity of the anode is plotted in Figure 7 as a relative transmissivity. It is normalized to 1 at 6500 Å for the red sensitive tube. The wavelength range of the plasmascope is about 3300 Å to 10,500 Å.

The auxiliary bench for the iron arc was mounted on a movable table to allow more flexibility in other experiments.

We have already taken sample spectrograms in argon and hydrogen and are planning quantitative studies of these gases in the next reporting period.

The studies in hydrogen require additions to our computer program library. We are therefore modifying some of our existing programs to apply to any gas, to be of standard notation and input, and to include the methods of determining the electron temperature and density using the hydrogen continuum.

We also have available a multi-channel Dymec integrating digital voltmeter with print out which will reduce data evaluation time.

Preliminary Experiments in Hydrogen Atmosphere

Tests in a hydrogen atmosphere revealed that there is only a limited parameter range in which this arc can be operated. The steady mode of operation is only permissible at very low pressures ($<$ 20 mmHg) where the anode arc attachment occurs in a rather diffused manner. With increasing pressure the anode arc attachment is more constricted and an intolerable amount of copper is evaporated from the anode at the arc terminus. This effect can be observed with the bare eyes because the predominant red radiation (H_{α}) of the visible hydrogen spectrum turns to green which is characteristic for copper. In addition, the anode surface appears eroded. The transition from the steady mode to the fluctuating mode occurs at about 150 mmHg at the highest attainable flow velocity. Therefore, the lower limit for the pressure parameter is about 150 mmHg.

In the higher pressure and flow velocity range difficulties arise from the limited open-circuit voltage of our present power supply. The field intensity required for a hydrogen arc is much higher than for an argon arc. In addition the volt-amp characteristic of a hydrogen arc exhibits a very steep slope in the low current range so that arc operation becomes rather unstable in this range. For a stable operation at low currents ($80 < I < 150$ Amp) the arc voltage may only reach about 50% of the open-circuit voltage which is presently only 160 volts. The maximum permissible pressure at the lowest flow velocity required for maintaining the fluctuating mode was about 350 mmHg.

The arc was struck in a pure argon atmosphere. By alternately evacuating and bleeding in hydrogen, the arc atmosphere was gradually changed to pure hydrogen. The purity was checked spectroscopically. No detectable argon lines or other impurities could be found after repeating the above process about 15 times.

A high speed Fastax film showed essentially the same arc behavior as experienced when using argon as the working fluid. However, the flow velocity required for the fluctuating mode and therefore the speed of the anode arc terminus were much higher, and the resolution of the arc movement with a camera speed of 5000 frames/sec was no longer satisfactory. The time interval τ required for one cycle of the moving arc became equal or even shorter than the time interval between two frames of the Fastax film.

In Figure 8 a still picture of the hydrogen arc is shown which was taken with an exposure time of 10^{-3} sec. Because of the fast movement of the anode arc terminus and the relatively long exposure time, streaks appear in the downstream part of the arc.

"Local" Heat Transfer Measurements to the Anode Using the Segmented Anode

During this period a second segmented anode especially designed for "local" heat transfer measurements was constructed. The energy transfer to each segment was determined calorimetrically by measuring the temperature rise of the cooling water with two thermocouples connected differentially and the water flow rate. A total of 22 thermocouples were installed in the anode. Each of these thermocouples was individually calibrated. From our previous experience with the fluctuating mode of the arc, any unshielded circuit will have large induced disturbances in it. Therefore, shielded thermocouples, which are commercially available, were used. The thermocouple leads and switches were enclosed in a grounded metal manifold.

Approximately 25 sets of data were taken with various parameter settings. The total energy transfer to the anode, obtained by summing up the heat transfer to each segment, compared favorably with the previous measurements taken with the nonsegmented anode. The total energy balances, however, did not close within the desired accuracy. Therefore, no data are included in this report. It is planned to repeat these measurements during the following reporting period.

PROPOSED WORK

The eighth quarter of the contracting period will be devoted primarily to the following tasks:

1) Completing "local" heat transfer measurements to the anode using the segmented anode.

2) Spectroscopic measurements using argon and hydrogen as the working fluid.

3) Determination of the temperature distribution downstream of the arc by using a thermocouple probe.

4) Testing of the double anode.

5) Overall energy balances using cylindrical anodes.

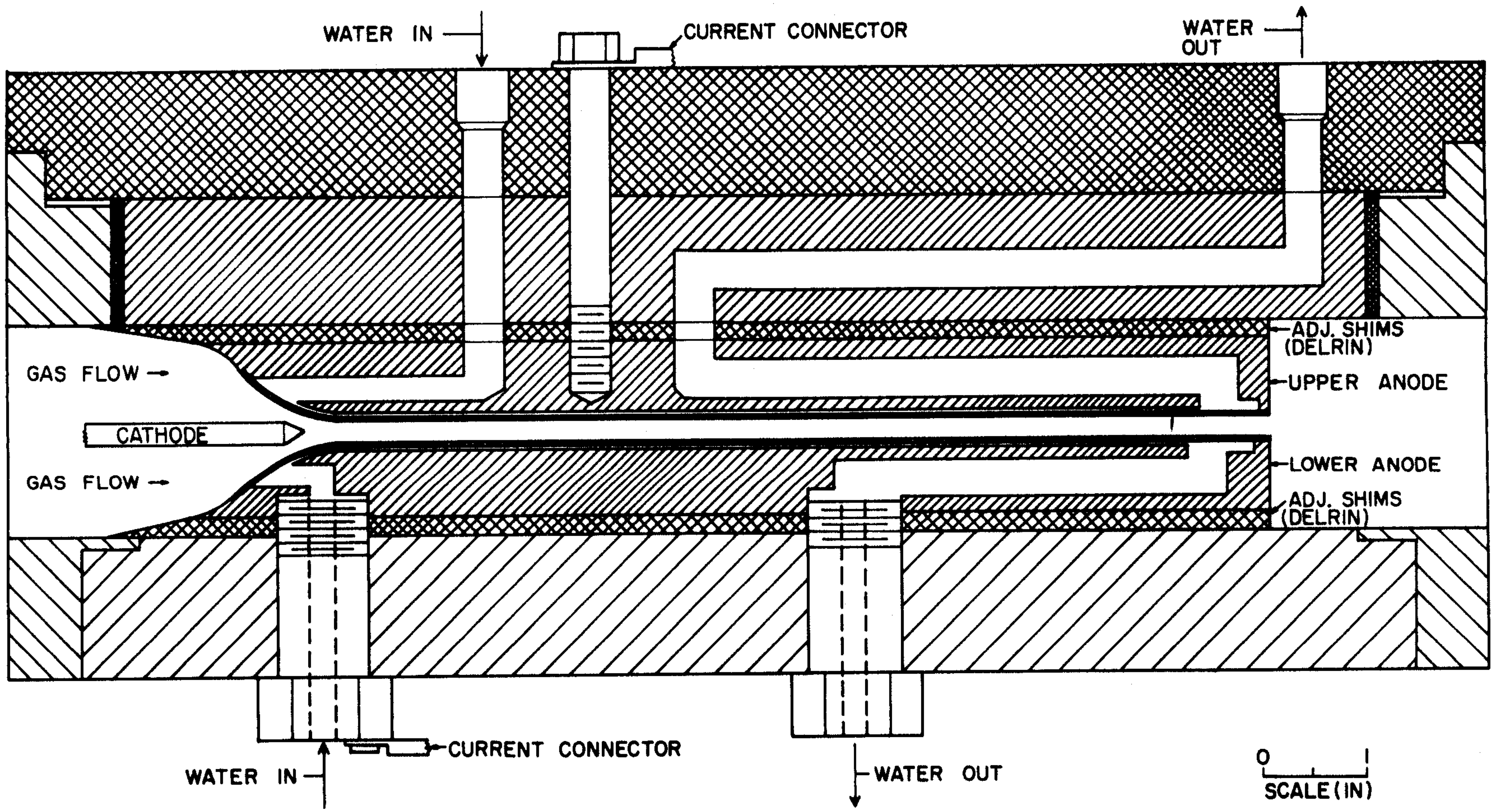

CROSS SECTIONAL VIEW OF THE PLANE, DOUBLE ANODE CONFIGURATION

FIG. 1:

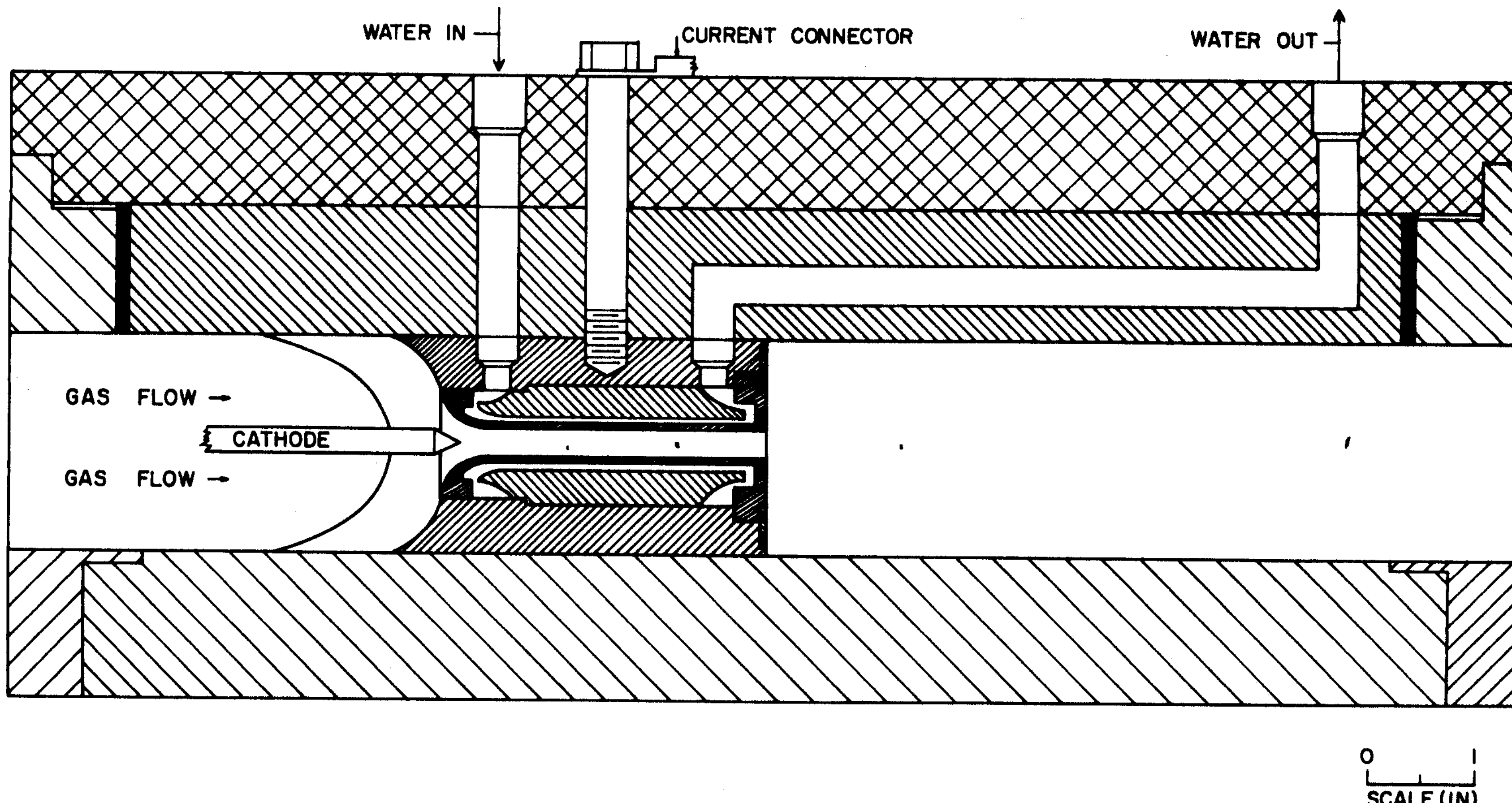

CROSS SECTIONAL VIEW OF THE CYLINDRICAL ANODE CONFIGURATION

FIG. 2:

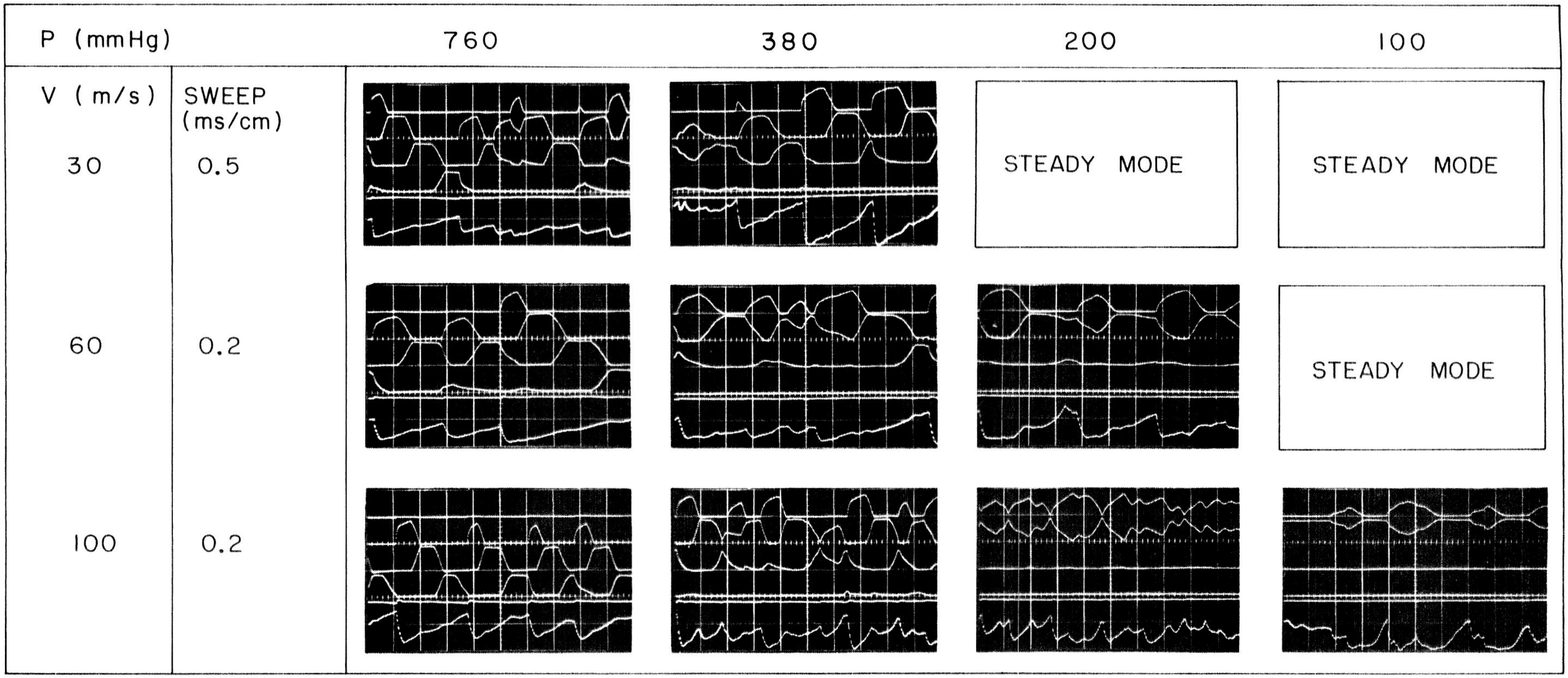

FIG. 3 TIME DEPENDENCE OF THE CURRENT DISTRIBUTION FOR THE SEGMENTED ANODE

ARGON I = 100 Amps, S = 7 mm

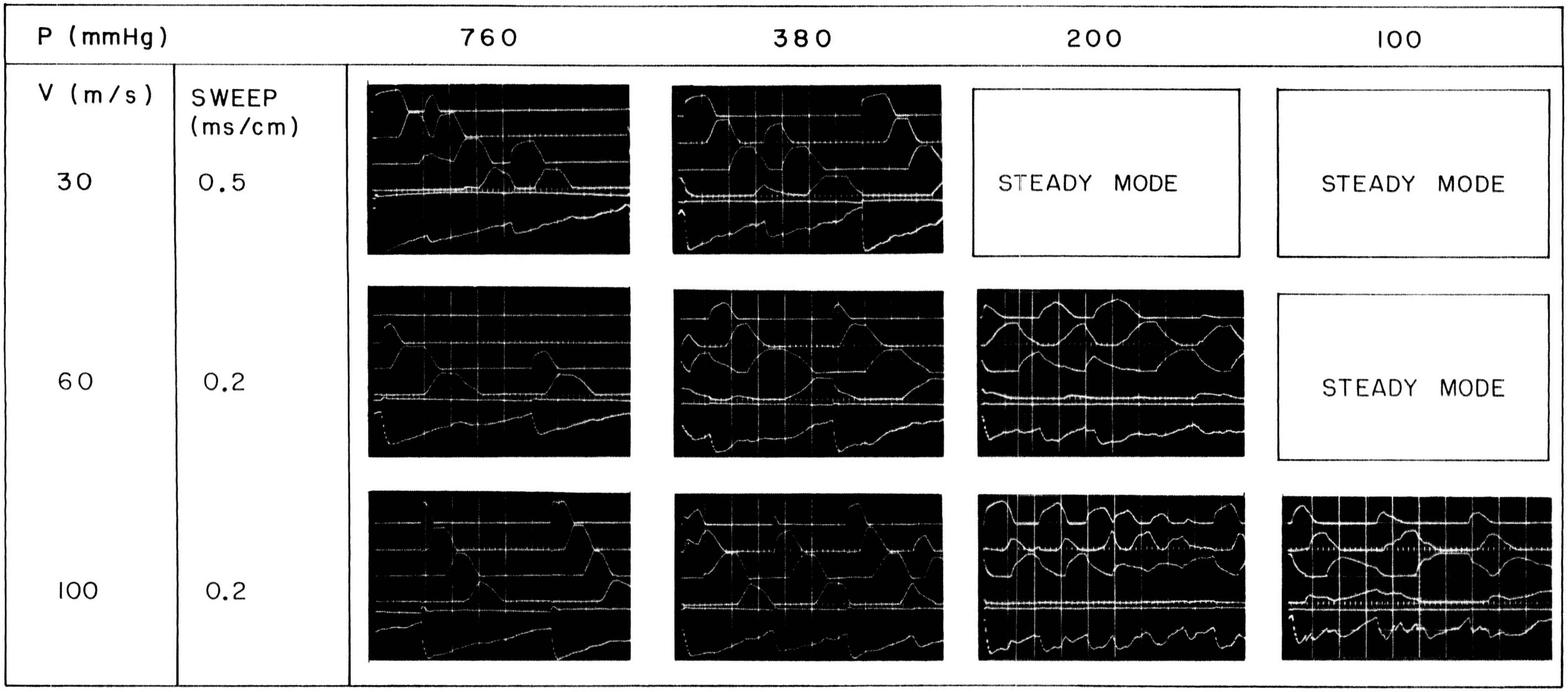

FIG. 4 TIME DEPENDENCE OF THE CURRENT DISTRIBUTION FOR THE SEGMENTED ANODE

ARGON I = 100 Amps, S = 8 mm

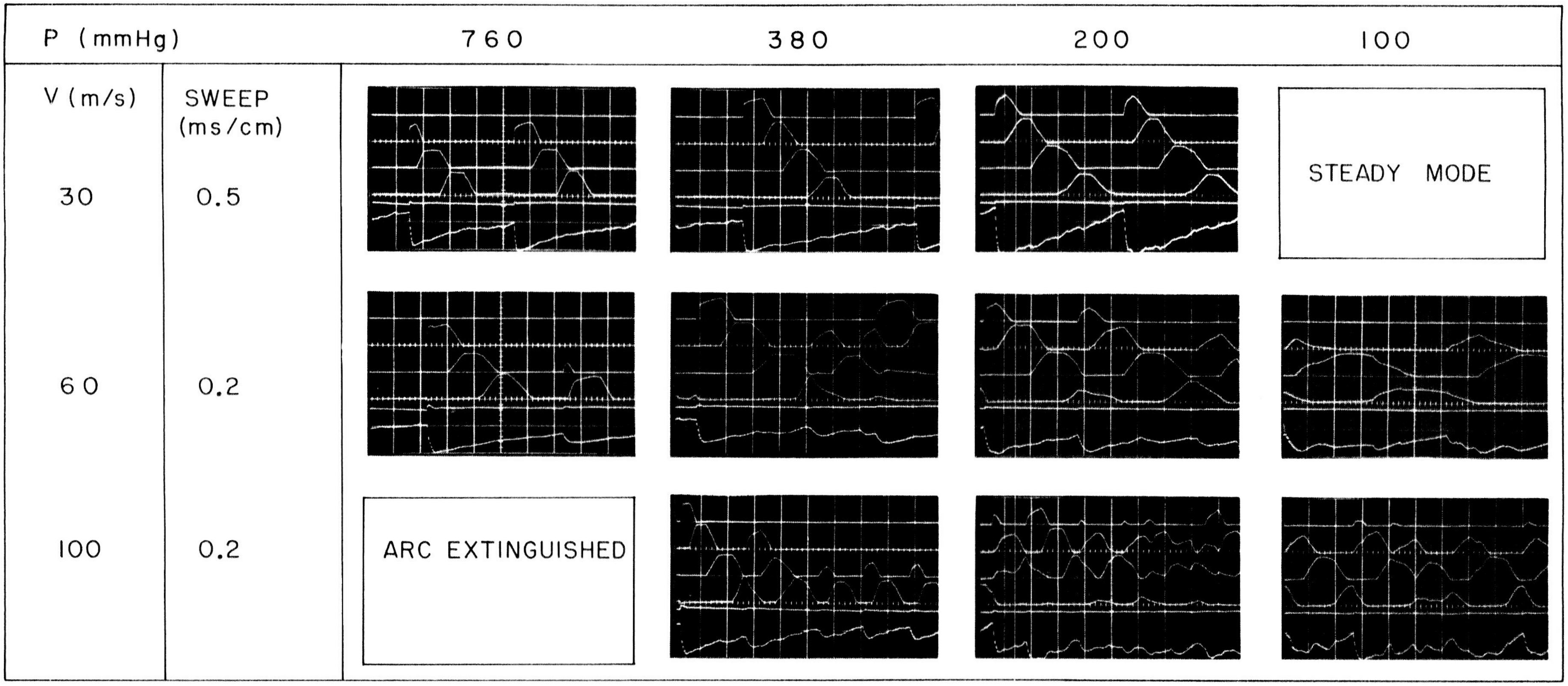

FIG. 5 TIME DEPENDENCE OF THE CURRENT DISTRIBUTION FOR THE SEGMENTED ANODE
ARGON I = 100 Amps, S = 9 mm

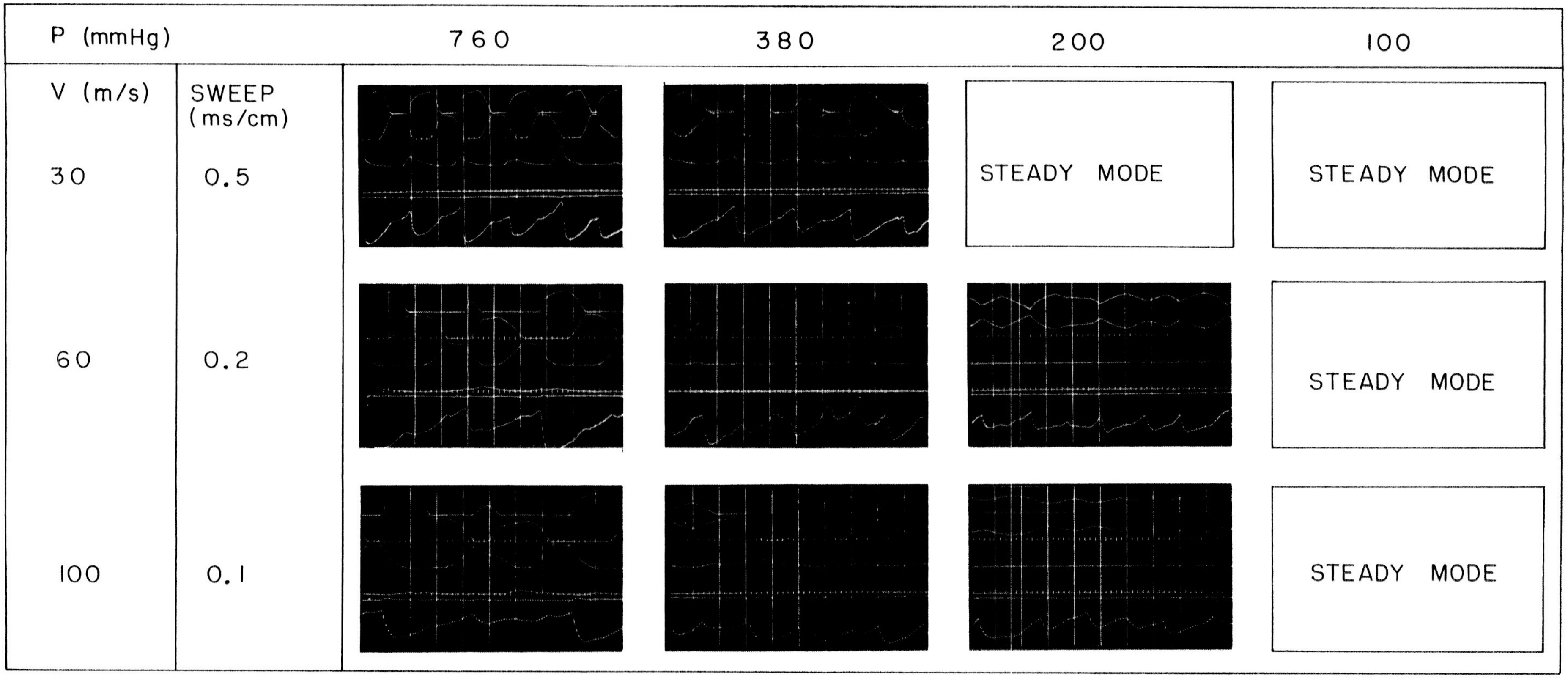

FIG. 6 TIME DEPENDENCE OF THE CURRENT DISTRIBUTION FOR THE SEGMENTED ANODE

ARGON $I = 200$ Amps, $S = 7$ mm

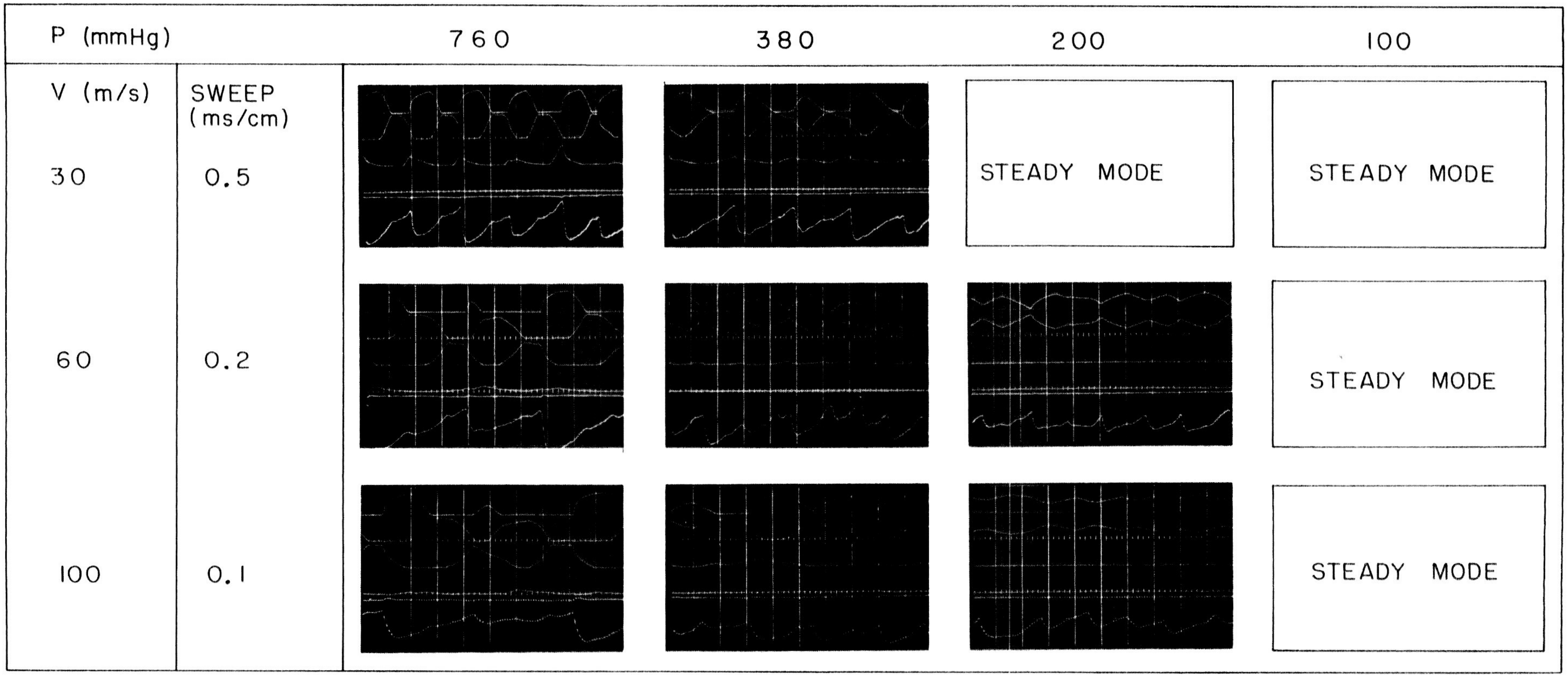

FIG. 6 TIME DEPENDENCE OF THE CURRENT DISTRIBUTION FOR THE SEGMENTED ANODE

ARGON I = 200 Amps, S = 7 mm

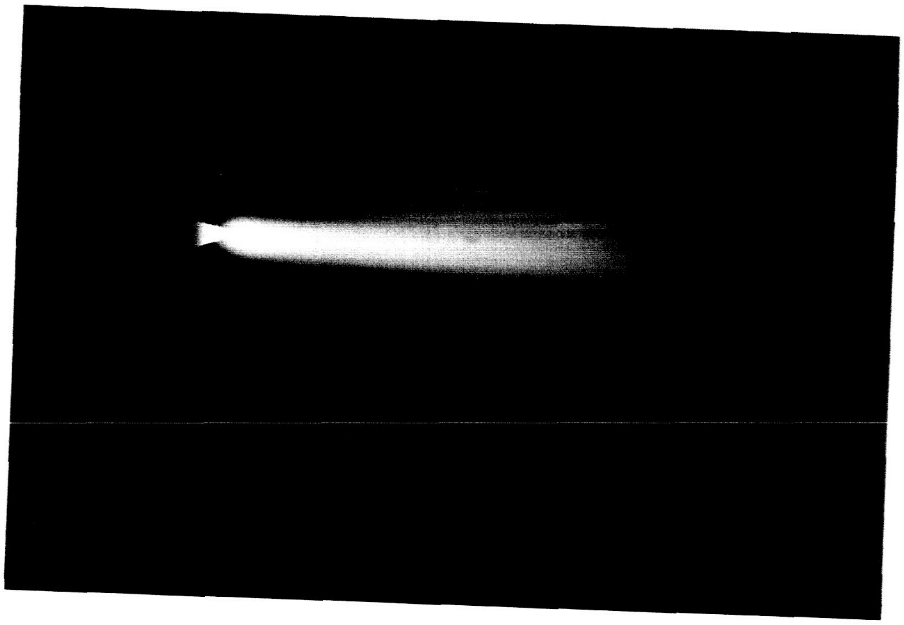

I = 120 Amp; U = 55 Volt; S = 5 mm
P = 250 mmHg; V $\cong$ 290 m/sec
Exposure time = 1/1000 sec

Fig. 8: Arc in Pure Hydrogen Atmosphere Operated in the Arc Tunnel

8	NASA Headquarters FOB - 10B 600 Independence Avenue, Northeast Washington, D C 20546 Attention: RNT/James Lazar	2
9	Commander/Aeronautical Systems Division Wright-Patterson AFB, Ohio Attention: AFAPL (APIE)/Robert Supp	1
10.	Thermo-Mechanics Research Laboratory OAR, USAF Wright-Patterson AFB, Ohio Attention: Mr. E Soehngen	1
11.	AFWL Kirtland Air Force Base, New Mexico Attention: WLPC/Capt C. F Ellis	1
12	Aerospace corporation P. O. Box 95085 Los Angeles, California 90045 Attention: Library Technical Documents Group	1
13	Westinghouse Astronuclear Laboratories Electrical Propulsion Lab. Pittsburgh, Pennsylvania 15234 Attention: Mr H W Szymanowski	1
14	Air Force Materials Laboratory MHYT Wright-Patterson AFB, Ohio 45433 Attention: E J Rolinsk	1

REVISED DISTRIBUTION LIST FOR QUARTERLY REPORTS

Addressee	Number of Copies
1. NASA-Lewis Research Center Spacecraft Technology Division 21000 Brookpark Road Cleveland, Ohio 44135 Attention: James Sovey J. Howard Childs	 5 2
2. NASA-Lewis Research Center Spacecraft Technology Procurement Section 21000 Brookpark Road Cleveland, Ohio 44135 Attention: John H. DeFord	 1
3. NASA-Lewis Research Center 21000 Brookpark Road Cleveland, Ohio 44135 Attention: Library Report Control Office Technology Utilization Office	 2 1 1
4. NASA-Lewis Research Center Electromagnetic Propulsion Division 21000 Brookpark Road Cleveland, Ohio 44135 Attention: John R. Jack	 1
5 NASA-Ames Research Center Moffett Field, California 94035 Attention: Dr. Glenn Goodwin	 1
6. NASA-Marshall Space Flight Center M-RP Bldg. 4484 Huntsville, Alabama 35812 Attention: Kalus Shocken	 1
7. NASA Scientific and Technical Information Facility Box 5700 Bethesda, Maryland 20014 Attention: NASA Representative/RQT-2448	 6